 doi:10.20944/preprints202101.0362.v1

Influence of north-easterly monsoon on carbonaceous particles and polycyclic aromatic hydrocarbons in $PM_{2.5}$ in the City of Kuala Lumpur, Malaysia

Hamidah Suradi[1], Md Firoz Khan[1,2*], Nor Asrina Sairi[1], Haasyimah Ab Rahim[1], Sumiani Yusoff[3], Yusuke Fujii[4], Qin Kai[2], Md. Aynul Bari[5], Murnira Othman[6], Mohd Talib Latif[7]

[1]Department of Chemistry, Faculty of Science, University of Malaya, 50603 Kuala Lumpur, Malaysia

[2]School of Environment Science and Spatial Informatics, China University of Mining and Technology, Xuzhou, China

[3]Institute of Ocean and Earth Environmental (IOES), University of Malaya, Kuala Lumpur 50603, Malaysia

[4]Department of Sustainable System Sciences, Graduate School of Humanities and Sustainable System Sciences, Osaka Prefecture University, 1-1 Gakuen-cho, Naka-ku, Sakai, Osaka, 599-8531, Japan

[5]Department of Environmental & Sustainable Engineering, College of Engineering and Applied Sciences, University at Albany, State University of New York, Albany, NY 12222, USA

[6]Institute for Environment and Development, Universiti Kebangsaan Malaysia, 43600 Bangi, Selangor, Malaysia

[7]Department of Earth Sciences and Environment, Faculty of Science and Technology, Universiti Kebangsaan Malaysia, 43600 Bangi, Selangor, Malaysia

 doi:10.20944/preprints202101.0362.v1

*Corresponding author: mdfirozkhan@um.edu.my; mdfiroz.khan@gmail.com (MF Khan)

Abstract

With increasing interest in understanding contribution of secondary organic aerosol (SOA) to particulate air pollution in urban areas, an exploratory study was carried out to determine levels of carbonaceous aerosols and polycyclic aromatic hydrocarbons (PAHs) in the City of Kuala Lumpur, Malaysia. $PM_{2.5}$ samples were collected using a high-volume sampler for 24 h in several areas in Kuala Lumpur during the north-easterly monsoon from January to March 2019. Samples were analysed for water soluble organic carbon (WSOC), organic carbon (OC), elemental carbon (EC) and secondary organic carbon (SOC) in $PM_{2.5}$ was estimated. Particle-bound PAHs were analysed using gas chromatography-flame ionization detector (GC-FID). Average concentrations of WSOC, OC and EC were 2.7 ± 2.2 (range of 0.63-9.1) µg/m^3, 6.9 ± 4.9 (3.1-24.1) µg/m^3 and 3.7 ± 1.6 (1.3-6.8) µg/m^3, respectively, with estimated average SOC of 2.3 µg/m^3, contributing 34% to total OC. The average of total PAHs was 1.8 ± 2.7 ng/m^3. Source identification methods revealed natural gas and biomass burning, and urban traffic combustion as dominant sources of PAHs in Kuala Lumpur. To understand human health risk posed by PAHs, a deterministic screening health risk assessment was also conducted for several age groups including infant, toddler, children, adolescent and adult. The total concentration of BaP_{eq} is 3.8 ng/m^3, with the average of 0.29 (range of 0.001-1.6) ng/m^3. Carcinogenic and non-carcinogenic risk of PAH species were well below the acceptable levels recommended by the USEPA. Future work is needed using long-term monitoring data to understand the origin of PAH contributing to SOA formation and to apply source-

 doi:10.20944/preprints202101.0362.v1

risk apportionment to know better the potential risk factors posed by the various sources in urban areas in Kuala Lumpur.

Keywords: Elemental carbon; Secondary organic carbon; Health impact; Polycyclic aromatic hydrocarbon; Northeasterly monsoon

Highlights

- Organic carbon was originated by 34% from secondary sources
- Dibenzo(a,h)anthracene (B[h]A) and indeno(1,2,3-cd)pyrene (I[c]P) are predominant PAHs
- Natural gas and biomass burning, and fuel combustion are the potential sources of PAHs
- A precautionary measure may help to reduce the PAHs exposure

1. Introduction

Urban air pollution is a potential cause for deleterious impact on public health and the environment. Several studies reported that there are excess death or global premature death in the urban and industrial areas due to air pollution [1-3]. The major causes of ambient air pollution are related to the rise in population, industrial activities and number of vehicles in cities [4-7].

Being a tiny air particles, $PM_{2.5}$ with an aerodynamic diameter equal to or less than 2.5 µm can easily penetrate deep into the human respiratory system [8] and showed an influence on the increase of daily mortality and morbidity to adults due to having

Preprints (www.preprints.org) | NOT PEER-REVIEWED | Posted: 18 January 2021 doi:10.20944/preprints202101.0362.v1

breathing difficulties and development of lung cancer [9]. While originating from primary and secondary sources [10], meteorological factors significantly influence $PM_{2.5}$ concentration at local and regional scale due to its smaller in size and ability to be transported in long range [11]. Previous studies have found north-easterly monsoon playing an important role on the high concentration of the air pollutants in Kuala Lumpur and neighbouring cities [12-15].

Particulate matter consists of different chemicals. The major chemical compositions in $PM_{2.5}$ are elemental carbon (EC) and organic carbon (OC) emits predominantly from the transportation sector, ammonium sulfate and ammonium nitrate, and inorganic mineral components [10,16]. EC is originated from the primary sources via the incomplete combustion processes whereas OC can come from both primary and secondary pathways [16]. Increasing the secondary organic aerosol (SOA) contribution to urban particulate air pollution has been well reported in the literature [17-19]. Gas-phase low volatile PAHs are also a significant source of SOA [18,19]. Secondary organic carbon (SOC) contributes significantly to the total particulate matter in the lower atmosphere. Water soluble organic carbon (WSOC) which is a part of SOC are also form via photochemical reaction of volatile organic carbon and this WSOC influence the cloud formation [17]. All these carbonaceous compounds consist of carcinogenic pollutants such as polycyclic aromatic hydrocarbons (PAHs) have potential to cause cancer.

PAHs are environmentally persistent organic pollutants (POPs) that consisted of two or more fused benzene rings [4,5,10]. According to Liu et al. Liu, Man, Ma, Li, Wu and Peng [9], the PAHs concentration is being higher in the respirable fraction of air particles than the larger fractions. PAHs are ubiquitous and semi-volatile that are released into ambient air through the incomplete combustion of organic materials. Several studies reported that the predominant emission sources of PAHs are automobiles, industrial processes, domestic heating systems, waste incineration facilities, tobacco smoking and several natural

sources including forest fires and volcanic eruptions [4,6,20-24]. Previous literatures reported that vehicle emission, coal burning and biomass combustion were principal sources of PAHs in $PM_{2.5}$ [25-27]. PAHs sources can be classified into two main groups such as pyrogenic and petrogenic. Pyrogenic PAHs are formed from incomplete combustion of organic matter such wood burning, coal combustion, natural gas and traffic related pollution, whereas petrogenic is related to direct contamination such as crude oil spillage [4,20,28]. In urban area, pyrogenic sources are the main source of PAHs especially high molecular particulate PAHs are mainly found in $PM_{2.5}$. Human exposure to PAHs may occur via inhalation, ingestion and dermal from air particles. However, the exposure of PAHs from inhalable tiny particles is significantly occurred via inhalation [29-31]. PAHs in $PM_{2.5}$ have attracted great concerns and have been widely studied due to their toxicity and damage to human health [27,32].

Due to the limited study on PAHs in $PM_{2.5}$, there is a knowledge gap on the emission, chemical profiles, toxicity effect and human exposure of this persistent class of organic pollutants. There is necessity to determine the potential sources and health risk estimation of PAHs in $PM_{2.5}$ especially in urban area. The U.S.EPA screening health risk assessment have been applied by several researchers in previous studies [4,5,7,9,22,31,33-35]. As seen the impact of PAHs towards human health, identifying the sources of them is crucial to mitigate the emission rate in ambient air. Principal component analysis-multiple linear regression (PCA-MLR) is one of receptor model that can be used to quantify the possible sources of PAHs in atmospheric particles by identifying the number of factors and the special profile of each sources [21,36,37]. There are many methods to determine the source apportionment that has been used by previous studies, such as positive matrix factorization (PMF) Sulong, Latif, Sahani, Khan, Fadzil, Tahir, Mohamad, Sakai, Fujii and Othman [35] and PCA Jamhari, Sahani, Latif, Chan, Tan, Khan and Tahir [37]. In this study, source

Preprints (www.preprints.org) | NOT PEER-REVIEWED | Posted: 18 January 2021 doi:10.20944/preprints202101.0362.v1

apportionment was done using PCA-MLR coupled with absolute principal component scores (APCS) due to its simplicity and high reliability.

Due to concern of adverse health effect of PAHs in urban environment at fine particulate size, an exploratory study was done to understand sources and health risk of PAHs at Kuala Lumpur City. The objectives of this study are to a) determine concentrations of WSOC, OC and EC and estimate the concentration of SOC in $PM_{2.5}$, b) investigate levels and potential sources of PAHs in $PM_{2.5}$ in selected Kuala Lumpur urban areas, c) estimate the potential health risk posed by PAHs species.

2. Methodologies

2.1 Study areas

Kuala Lumpur is the federal capital of Malaysia that has high density of population and is a centre of commercial activities and surrounded with industrial activities with high traffic density. The volume of road traffic is higher during peak hours every day and this traffic increases rapidly during public holiday. Yet, its population has exceed one million (1,453,975 people) as reported by Wordometers Worldometers [38]. The samples were collected at three different buildings namely Kuala Lumpur Health Clinic (KKKL) (Lat 3.172127°, lon 101.704343°), Wisma SCA (WISMA) (lat 3.132627°, lon 101.712559°) and Kuala Lumpur City Hall (DBKL) (lat 3.151950°, lon 101.694410°) as shown in **Fig. S1**. KKKL is a public medical center in Kuala Lumpur, and this area is near with schools. WISMA is a building that is surrounded with shops and DBKL is the city council which administers the city of Kuala Lumpur in Malaysia. All these sampling areas are located near to the main routes that are very busy and have high density of traffic. In addition,

Preprints (www.preprints.org) | NOT PEER-REVIEWED | Posted: 18 January 2021 doi:10.20944/preprints202101.0362.v1

these areas are places that all age group of people visits and therefore, they are exposed to PAHs pollution.

2.2 Local meteorology and transport of air mass

Kuala Lumpur is located at 56 m above sea level. In the middle of March 2019, the change of ambient temperature was higher compared to January and February as shown in **Fig. S2**. Interestingly, relative humidity inversely changes to ambient temperature. The local meteorology data was taken from Subang Airport (www.wunderground.com) located at the about 20 km from Kuala Lumpur. The synoptic level of wind impacts greatly the ambient level of pollutants over Malaysia. As shown in **Fig. 1**, a stronger wind during January was blowing from the South China Sea (north-easterly monsoon) compared to February and March. This strong wind carries higher pollutants as well as water vapor from the ocean to Malaysia and causes heavy rainfall. The synoptic level wind vector of the assimilated data was downloaded from ECMWF data repository (European Centre for Medium-Range Weather Forecasts) and plotted using Grid Analysis and Display System (GrADS) software. **Fig. 2** shows the monthly cluster of backward trajectories (BTs) constructed using Hybrid Single-Particle Lagrangian Integrated Trajectory version 4.9 (Hysplit 4.9). The BTs were calculated using a set of reanalysis data by NCEP/NCAR (ftp://arlftp.arlhq.noaa.gov/pub/archives/reanalysis) calculated daily on 00, 06, 12, 18 UTC, 500 m as releasing height, 6 h interval and 120 h as total travel time. Then, the estimated cluster data were plotted in an Igor Pro platform (WaveMetrics, OR, USA).

Preprints (www.preprints.org) | NOT PEER-REVIEWED | Posted: 18 January 2021 doi:10.20944/preprints202101.0362.v1

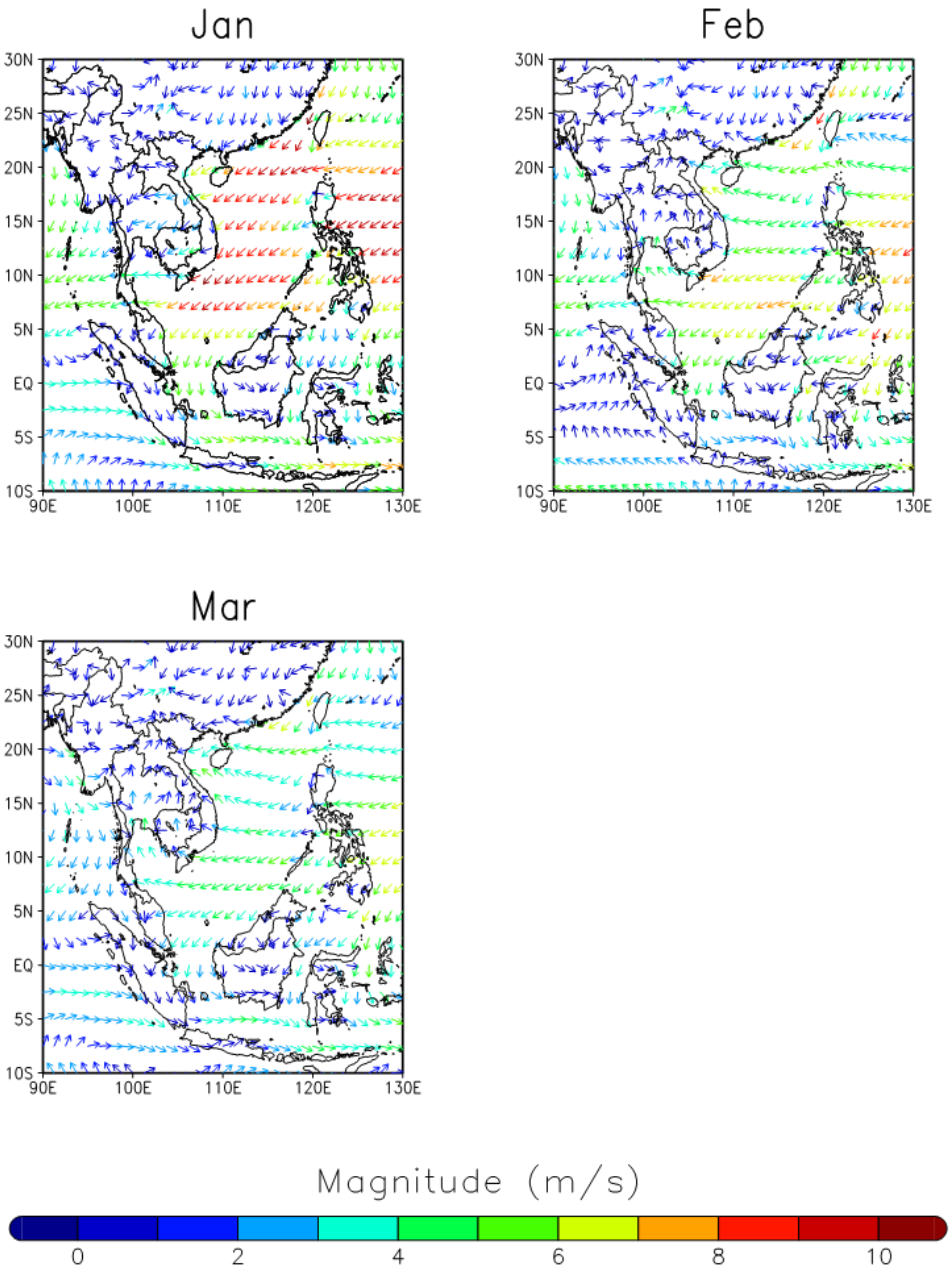

Figure 1: Synoptic wind flow from January 2019 until March 2019.

Preprints (www.preprints.org) | NOT PEER-REVIEWED | Posted: 18 January 2021 doi:10.20944/preprints202101.0362.v1

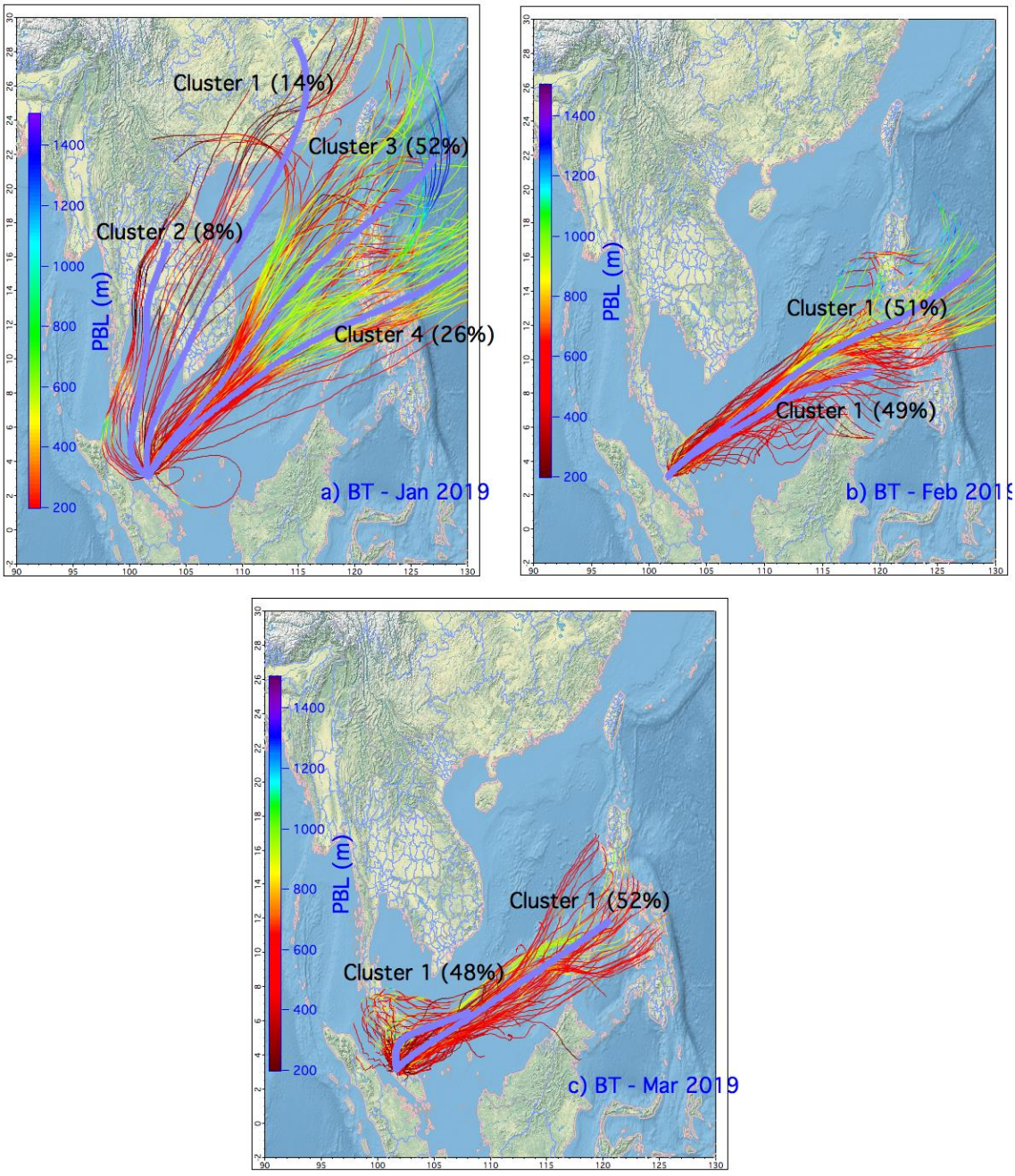

Figure 2: Cluster of backward trajectories during January, February and March 2019

2.3 Air sampling procedures

$PM_{2.5}$ samples were collected on quartz fibre filters using a Tisch high volume sampler (Tisch Environmental, USA). Samples were collected over 24 h (12:00 am to 12:00 am (+ 1 day)) from January to March 2019 at three different locations in Kuala Lumpur which were KKKL, WISMA and DBKL. For each of the locations, two samples were selected in each month with total of eighteen samples all together. The flowrate for all the samples were presented in **Table S1** in supplementary file. After samples collection, the filters

Preprints (www.preprints.org) | NOT PEER-REVIEWED | Posted: 18 January 2021 doi:10.20944/preprints202101.0362.v1

were wrapped with aluminium foil and stored at -25 °C prior to further extraction of PAHs was being performed.

2.4 Analysis of OC and EC and estimation of secondary organic carbon (SOC)

The carbonaceous contents of $PM_{2.5}$ were quantified using OC-EC carbon analyser (Sunset Laboratory Inc., USA), which employs thermal optical reflectance [39] following the IMPROVE_A protocol. The IMPROVE_A temperature defines temperature plateaus for thermally-derived carbon fractions as follows: 140 °C for OC1, 280 °C for OC2, 480 °C for OC3, 580 °C for OC4 and OP (splitting of OC and EC) in presence of helium (He) carrier gas; 580 °C for EC1, 740 °C for EC2 and 840 °C for EC3 in a mixture of 98% He and 2% oxygen carrier gas. From the eight carbon fractions, OC, EC, and total carbon (TC) were calculated as follow in Eq.1, Eq.2 and Eq.3 as described by the Sunset IMPROVE_A protocol and reported by Fujii, *et al.* [40],Khan, *et al.* [41]:

$$OC = OC1 + OC2 + OC3 + OC4 + OP \quad (1)$$

$$EC = EC1 + EC2 + EC3 - OP \quad (2)$$

$$TC = OC + EC \quad (3)$$

where OP (the amount of pyrolyzed OC) is defined as the carbon content measured after the introduction of O_2 until reflectance returns to its initial value at the start of analysis.

By using the lowest ratio value of OC to EC (OC/EC), the secondary organic carbon (SOC) concentrations can be estimated. The SOC concentrations were calculated as follow [42,43] in Eq. 4 :

$$SOC = OC - \left[\left(\frac{OC}{EC}\right)_{min} \times EC\right] \quad (4)$$

where the minimum OC/EC ratio $((OC/EC)_{min})$ is believed to be the value for primary $PM_{2.5}$ emission source and season dependent, which has significant ranges of uncertainty.

Preprints (www.preprints.org) | NOT PEER-REVIEWED | Posted: 18 January 2021 doi:10.20944/preprints202101.0362.v1

The sampling was conducted strategically on 24 h basis and the north-easterly monsoon which potentially reduce the uncertainty in the concentration. Khan et al. Khan, Sulong, Latif, Nadzir, Amil, Hussain, Lee, Hosaini, Shaharom and Yusoff [41],Khan, *et al.* [44] stated that, the lowest value of EC/OC was used to represent the primary combustion source.

2.5 Analysis of water-soluble organic carbon (WSOC).

A 2×2 cm of filter sample was cut and placed inside a beaker. Then, 50 mL of ultrapure water are added into the beaker and the sample with ultrapure water was sonicated for 20 minutes. After sonication, the mixture was filtered using Whatmann filter paper 100 mm in diameter. The method was repeated for three blank filters and for all samples. Then, all the blank and sample solutions were analysed using Total Organic Carbon Analyzer (TOC-L, Shimadzu, Japan) to determine WSOC concentrations. This methodology was adopted from Thuy et al. Thuy, *et al.* [45].

2.6 Extraction procedures for PAHs in $PM_{2.5}$ samples

2.6.1 Extraction of the PAHs composition using magnetic nanoparticles.

For analysis, the filter paper was cut into one quarter or half of the filter sample and placed inside a beaker. The exposed filter was extracted using ultrasonic agitation (10 minutes sonication time) using 25 mL of dichloromethane (DCM) as solvent. Then, modified magnetic nanoparticles (C_8MNPs) were added immediately into the extraction solution and then sonicated for five minutes. The detailed information of C_8MNPs has been described in the supplementary file. Theoretically, the PAHs that were extracted out clean up via adsorption on the C_8MNPs. The adsorption efficiency has been tested using the recovery analysis of spiking known standard of PAHs. After that, with the help of an external magnetic field, the solution was settled down until its clear. The DCM was thrown away and washed with DCM three times. Next, a 200 µL of n-hexane was added to the PAHs adsorbed on C_8MNPs and sonicated for 10 minutes. PAHs were dissolved in n-hexane. Then, the n-hexane was separated from the magnetic nanoparticles with the

Preprints (www.preprints.org) | NOT PEER-REVIEWED | Posted: 18 January 2021 doi:10.20944/preprints202101.0362.v1

help of an external magnetic field, collected and placed inside GC vial. The method reported here is slightly modified from the study published by Soo et al. [46].

2.7 Analysis of PAHs using Gas Chromatography-Flame Ionization Detector (GC-FID)

2.7.1 Preparation of calibration standard

A standard mixture of PAHs was used to construct the calibration curves. There are eighteen PAHs in the standard mixtures, and each compound eluted at different retention times, following the elution order based on their boiling point.

The standard solution of 0.2 ppm, 0.5 ppm, 1.0 ppm, 2.0 ppm and 3.0 ppm of PAHs mixtures were prepared. From the standard solution, calibration curve of peak area against concentration were plotted for each PAH compound. Equation from the calibration curve for each compound were used to determine the concentration of PAHs for all samples.

2.7.2 Determination of PAHs using GC-FID

The extracted samples were analysed using Gas Chromatography-Flame Ionization Detector (GC-FID) (Agilent Technologies 7890A, GC System, USA). A capillary column (HP-5, Agilent, USA) of length 30 m, internal diameter (id) 0.320 mm and thickness 0.25 µm was used. N_2 is used as make up gas at the flow rate of around 25 mL/min in GC/FID, while H_2 is used as carrier gas. The sample was injected in a splitless mode at 270 °C. The GC column temperature was programmed as 40 ºC as initial temperature, followed by temperature increases from 40 to 150 °C at 8 °C min^{-1} and from 150 to 310 °C at 4 °C min^{-1} and then isothermal at 310 °C for 10 minutes. Then, the peaks were identified for individual PAH based on the retention time (RT) and respective boiling point of the compounds. Each peak was identified by comparing them with the retention time from the standard solution. The PAHs concentrations were determined using the calibration curve of the standards.

Preprints (www.preprints.org) | NOT PEER-REVIEWED | Posted: 18 January 2021 doi:10.20944/preprints202101.0362.v1

2.8 Quality assurance and quality control (QA/QC)

As for the EC and OC analysis, a set of blank filters were examined and determined the thermally derived EC, OC and other fractions. The EC and OC of the samples were subtracted from the filter blanks. A similar step also followed for GC-FID analysis for PAHs. For EC, OC, and TOC analysis, concentration of all samples must be minus with the blank concentration. In FTIR analysis, baseline correction is done to remove the estimated baseline from the spectrum data and leave only the pure signal and some noises. The extraction of PAHs from $PM_{2.5}$ particles was validated through the spiking of 2 ppm of PAHs mixtures at the initial stage of the extraction using MNPs. The recovery of the PAHs was ranging from 61% to 166% for acenaphthene (Ace), 54% to 80% for Benzo (b) fluoranthene, 49% to 70% for Benzo (k) fluoranthene, Benzo (a) pyrene 46% to 61% and 103% to 118% for Dibenzo (a,h) anthracene.

2.9 Data analysis and modelling

2.9.1 Statistical analysis

Exploratory data analysis was performed for the PAHs and EC/OC results. The initial data analysis such as descriptive statistics, distribution and correlation were conducted using IBM Statistic SPSS (Version 25) and Microsoft Excel.

Preprints (www.preprints.org) | NOT PEER-REVIEWED | Posted: 18 January 2021 doi:10.20944/preprints202101.0362.v1

2.9.2 Diagnostic ratio (DR) and receptor modelling

2.9.2.1 Diagnostic ratio (DR)

In this study, the sources of the PAHs were estimated using diagnostic ratio. The PAHs particles can come from many possible sources as shown in **Table S2** that have been reported by other literatures [39,47-50].

2.9.2.2 Receptor modelling

Multivariate receptor modelling is very useful to perform source apportionment analysis in air pollution. Principal component analysis (PCA) in combination with multiple linear regression (MLR) has been applied to identify the potential sources of PAHs in $PM_{2.5}$. A number of research groups has been applied PCA-MLR in air pollution studies since decades [21,36,51,52].

In PCA, the input data was carefully screened and clean up the outliers, data below detection limit and the missing data was replaced with geometric mean of each variables. To reduce the variability in the concentration, a normalization procedure was followed through the deduction of the concentration from the average value and then divided with the standard deviation. The rescaled and normalized new database has been used for PCA procedure. Next, the key challenge is to obtain a suitable set of principal components (PC) factors. As for this step, we applied several options such as increase or decrease of the number of the factors, threshold of Eigen value, variance (%) and rotation of the PC loadings. An Eigen value is a mathematical term and to set a threshold of Eigen value 1 helps to know the variability to the PC factors. The variance (%) of the PCs may help to know the significance of the PCs. To obtained a minimum set of PCs with the largest of the variability, we applied all the steps described above [20,22,37]. Suitability of the PAHs samples for PCA analysis was tested using the Kaiser-Meyer-Olkin (KMO). A large value of KMO (close to one) generally reflected that the data set is suitable to carry out PCA

Preprints (www.preprints.org) | NOT PEER-REVIEWED | Posted: 18 January 2021 doi:10.20944/preprints202101.0362.v1

analysis while lower value of KMO indicates the less suitability of the data set for PCA analysis. Jamhari et al. Jamhari, Sahani, Latif, Chan, Tan, Khan and Tahir [37] stated that the KMO value of greater than 0.6 is required for the suitability of data set in PCA procedure. The value of KMO in this study is 0.650. This value is close to one, therefore, the data set is suitable for PCA analysis. Thus, PCA analysis was performed to identify the potential sources of the PAHs samples. To obtain the quantitative contribution of the identified sources, the PCA scores were corrected using absolute principal component scores (APCS) suggested by Thurston and Spengler (1985). Then, the APCS were regressed against the total PAHs concentration detected by GC-FID.

2.9.3 US EPA Health risk modelling

Health risk of PAHs exposure can be estimated via the pathways of ingestion, inhalation, or dermal exposure as suggested by USEPA [53]. However, in this study, inhalation of air particles contaminated with PAHs was considered for health risk assessment as $PM_{2.5}$ is aerodynamically very tiny and can penetrate the human respiratory system to the alveolar level. The Benzo(a)Pyrene equivalent health risk as B[a]Peq was determined using the equation below:

$$\mathrm{B[a]Peq} = \sum(\mathrm{C}_i \times \mathrm{TEF}) \quad (5)$$

Where C_i is the concentration of individual compound in each sample and TEF is toxic equivalency factors which has different value for each compound.

The excess lifetime cancer risk (ELCR) in humans and hazard quotient (HQ) can be determined by calculating the lifetime average daily dose (LADD) for carcinogenic and average daily dose for non-carcinogenic exposure of PAHs according to USEPA guidelines [54].

For LADD, the equation is:

Preprints (www.preprints.org) | NOT PEER-REVIEWED | Posted: 18 January 2021 doi:10.20944/preprints202101.0362.v1

$$\mathrm{LADD} = \frac{\mathrm{C}\times\mathrm{IR}\times\mathrm{ED}\times\mathrm{EF}}{\mathrm{BW}\times\mathrm{ALT}} \quad (6)$$

ELCR was calculate as follow:

$$\mathrm{ELCR} = \mathrm{LADD} \times \mathrm{SF} \quad (7)$$

Where, C is concentration in air particles (mg m^{-3}), IR is the air inhalation rate, EF is the exposure frequency, ED is the lifetime exposure duration, BW is the body weight, ALT is the averaging lifetime for carcinogens and SF is the slope factor (mg kg^{-1} $day^{-1})^{-1}$. SF can be determined as;

$$\mathrm{SF} = \mathrm{IUR} \times [\frac{1}{\mathrm{IR}}] \times \mathrm{BW} \quad (8)$$

where IUR is inhalation unit risk.

In this study, the health risk assessments are calculated for five group age; infant, toddler, children, adolescent and adult because these group are exposed to the PAHs pollution. The reference values for all the constant above shows in the **Table S3** and **Table S4** for IUR values.

Lifetime lung cancer risk (LLCR) can be calculated by multiplying the total B[a]Peq with 8.7×10^{-5} $(ngm^{-3})^{-1}$.

For non-carcinogenic exposure, the Hazard quotient (HQ) was calculated using ADD and reference dose (R_fD). ADD are calculated using based on Eq. (6).

$$\mathrm{HQ} = \frac{\mathrm{ADD}}{\mathrm{R_fD}} \quad (9)$$

The value of R_fD are different for every PAHs compound and has been referred in **Table S5**.

Preprints (www.preprints.org) | NOT PEER-REVIEWED | Posted: 18 January 2021 doi:10.20944/preprints202101.0362.v1

3.0 Results and Discussion

3.1 OC, EC and SOC

Concentrations of OC1, OC2, OC3, OC4, OP, EC1-OP, EC2 and EC3 are shown in **Fig. S6a**. Concentrations of OC, EC and TC in each filter samples are shown in **Fig. S6b** and OC to EC ratio for each filter samples are illustrated in **Fig. S5**. **Table 1** shows the statistical table for all the variables. From **Fig. S6a**, concentration of OC2, OC3 were high in filter samples on 17 March 19 from WISMA and DBKL. OC3 was about 44% of total OC and EC1-OP was about 92% of EC. The OP value was high in filter samples on 17 March 2019 also at WISMA and DBKL with value of 6.40 and 6.37 μg/m^3, respectively. Both of these filters have darkest colour of their filters, therefore their OC, EC, and OP concentration are relatively high compared to other filter samples. From **Table 1**, average concentrations of OC and EC were 6.88 ± 4.94 (range from 3.12-24.1) and 3.68 ± 1.58 (range from 1.32-6.82) μg/m^3, respectively, with an average OC/EC ratio of 1.86 (range from 1.24-3.53). Fujii, Iriana, Oda, Puriwigati, Tohno, Lestari, Mizohata and Huboyo [40] reported that the average OC/EC ratio for peatland and background were 36.4 ± 9.08 and 2.99 ± 0.74 respectively, for aerosols emitted from peatland fire in Riau, Sumatra, Indonesia. This value is larger than our results because the study is conducted near the peatland fire area, that emitted large amount of organic substances. Among the three sampling sites, Wisma has the highest concentration of OC with concentrations of 8.73 μg /m^3 followed by DBKL and KKKL with concentration of 6.99 μg /m^3 and 4.93 μg /m^3 respectively. Whereas for EC, DBKL has the highest concentration with value of 4.33 ± 1.46 μg /m^3 followed by Wisma (3.98 ± 1.76 μg /m^3) and KKKL (2.73 ± 1.25 μg /m^3).

Preprints (www.preprints.org) | NOT PEER-REVIEWED | Posted: 18 January 2021 doi:10.20944/preprints202101.0362.v1

Table 1: Carbonaceous fractions in $PM_{2.5}$ from three sites in Kuala Lumpur.

Variables	Sampling sites	Mean	Minimum	Maximum	Stdev.
OC1 (µg /m^3)	Overall	0.056	0.018	0.136	0.034
OC2 (µg /m^3)	Overall	1.68	0.687	4.60	1.02
OC3 (µg /m^3)	Overall	3.00	1.36	12.9	2.67
OC4 (µg /m^3)	Overall	1.43	0.527	4.25	1.04
OP (µg /m^3)	Overall	0.721	0.091	2.21	0.435
EC1-OP (µg /m^3)	Overall	3.40	1.10	6.40	1.56
EC2 (µg /m^3)	Overall	0.272	0.208	0.382	0.052
EC3 (µg /m^3)	Overall	0.007	0.0004	0.045	0.010
TC (µg /m^3)	Overall	10.6	4.61	30.9	6.26
OC (µg /m^3)	Overall	6.88	3.12	24.1	4.94
	DBKL	6.99	4.17	13.5	3.30
	Wisma	8.73	3.69	24.1	7.64
	KKKL	4.93	3.12	9.33	2.23
EC (µg /m^3)	Overall	3.68	1.32	6.82	1.58
	DBKL	4.33	2.76	6.58	1.46
	Wisma	3.98	2.53	6.82	1.76
	KKKL	2.73	1.32	4.33	1.25
OC/EC	Overall	1.86	1.24	3.53	0.626
	DBKL	1.60	1.24	2.04	0.343
	Wisma	2.01	1.28	3.53	0.820
	KKKL	1.95	1.24	3.04	0.649
SOC (µg/m^3)	Overall	2.33	-	15.6	3.61
	DBKL	1.64	-	5.32	1.97
	Wisma	3.81	0.13	15.6	5.87
	KKKL	1.56	0.020	3.98	1.43
TOC (µg/m^3)	Overall	2.73	0.627	9.12	2.17

From the EC and OC obtained, secondary organic carbon (SOC) was calculated by using the minimum ratio of OC to EC, which has value of 1.24. From **Table 1**, the average of SOC is 2.33 (range of 0.00 to 15.6) µg/m^3, which is 34% of total OC. In consequence, 66% of total OC are coming from primary combustion sources. Khan, Sulong, Latif, Nadzir, Amil, Hussain, Lee, Hosaini, Shaharom and Yusoff [41] reported that during the southeast dry season (southwest monsoon), estimated SOC was 85% of the total OC and the remaining 15% may have been released from primary combustion sources. These percentages are

Preprints (www.preprints.org) | NOT PEER-REVIEWED | Posted: 18 January 2021 doi:10.20944/preprints202101.0362.v1

different from our study because their study was conducted at semi urban area while our study was conducted at urban area of Kuala Lumpur. Photochemical oxidation increases during the summer time which is another region to show a higher value of OC/EC or SOC as suggested by Gao, *et al.* [55]. Among three sites, Wisma has the highest values of SOC with concentrations of 3.81 µg /m^3 followed by DBKL (1.64 µg /m^3) and KKKL (1.56 µg /m^3). Meaning that, Wisma produced more SOC in the atmosphere compared to Wisma and KKKL.

3.2 WSOC

The concentration of WSOC in $PM_{2.5}$ (µg/m^3) is shown in **Table S7**. The statistical table for TOC concentration is shown in **Table 1**. From this analysis, TOC mean concentration is 2.73 ± 2.17 (range of 0.63-9.12) µg/m^3 which is a measure of total water-soluble organic carbon (WSOC). This value is different with the mean concentration of total OC which is 6.88 ± 4.94 (range of 3.13-24.08) µg/m^3 although the filter samples are the same. This is because in this analysis, we only detected the concentration of organic carbon that was dissolved in water whereas in OC analysis, all the organic carbon in the filter samples was detected. This result was higher compared to previous study in Hanoi, Vietnam, that reported the concentration of WSOC in atmospheric nanoparticles were 1.51 (0.90-2.11) µg/m^3 and 0.41 (0.51-1.83) µg/m^3 in rainy season and dry season respectively (Thuy et al., 2017). Another study indicated higher concentration of WSOC in $PM_{2.5}$ compared to Kuala Lumpur [56].

3.3 Variation of PAHs

Out of 13 measured PAHs, dibenzo(a, h)anthracene (B[h]A) was predominant with mean concentration of 1.20 ng/m^3, followed by indeno(1,2,3-cd)pyrene (I[c]P), benzo [45] perylene (B[g]P), benzo(a)pyrene (B[a]P), benzo(a)anthracene (B[a]A), benzo(k)fluoranthene (B[k]F), acenaphthene (Ace) and benzo(b) fluoranthene (B[b]F) with mean concentration of 0.95, 0.72, 0.41, 0.39, 0.38, 0.33 and 0.30 ng/m^3 , respectively

Preprints (www.preprints.org) | NOT PEER-REVIEWED | Posted: 18 January 2021 doi:10.20944/preprints202101.0362.v1

as shown in **Table 2**. All these PAHs compounds have high molecular weight, high stability and cancer cause-potential.

Table 2: Summary statistics for the PAHs concentrations (mg/m^3) in the $PM_{2.5}$ samples.

	Compound	N	Mean	Min	Max	Stdev
Overall	Ace	3	3.27×10^{-7}	4.67×10^{-8}	6.41×10^{-7}	2.99×10^{-7}
	Flr	8	2.08×10^{-7}	3.63×10^{-8}	8.91×10^{-7}	3.04×10^{-7}
	Ant	10	2.33×10^{-7}	6.82×10^{-8}	1.06×10^{-6}	3.18×10^{-7}
	Flt	10	1.61×10^{-7}	4.71×10^{-8}	9.70×10^{-7}	2.86×10^{-7}
	Pyr	9	1.91×10^{-7}	4.05×10^{-8}	9.08×10^{-7}	2.91×10^{-7}
	B[a]A	5	3.94×10^{-7}	1.37×10^{-7}	9.57×10^{-7}	3.26×10^{-7}
	Chr	7	2.07×10^{-7}	1.18×10^{-7}	2.89×10^{-7}	5.60×10^{-8}
	B[b]F	12	3.03×10^{-7}	1.48×10^{-7}	3.79×10^{-7}	6.77×10^{-8}
	B[k]F	5	3.75×10^{-7}	2.85×10^{-7}	4.20×10^{-7}	5.21×10^{-8}
	B[a]P	4	4.06×10^{-7}	2.13×10^{-7}	5.82×10^{-7}	1.51×10^{-7}
	I[c]P	2	9.46×10^{-7}	8.10×10^{-7}	1.08×10^{-6}	1.93×10^{-7}
	B[h]A	1	1.20×10^{-6}	1.20×10^{-6}	1.20×10^{-6}	-
	B[g]P	1	7.15×10^{-7}	7.15×10^{-7}	7.15×10^{-7}	-
	Total PAHs	13	1.74×10^{-6}	1.48×10^{-7}	9.94×10^{-6}	2.68×10^{-6}
DBKL	Flr	1	6.43×10^{-8}	6.43×10^{-8}	6.43×10^{-8}	-
	Ant	2	1.16×10^{-7}	7.48×10^{-8}	1.58×10^{-7}	5.86×10^{-8}
	Flt	2	8.84×10^{-8}	5.77×10^{-8}	1.19×10^{-7}	4.35×10^{-8}
	Pyr	2	6.23×10^{-8}	4.48×10^{-8}	7.98×10^{-8}	2.48×10^{-8}
	B[a]A	1	2.38×10^{-7}	2.38×10^{-7}	2.38×10^{-7}	-
	Chr	1	2.42×10^{-7}	2.42×10^{-7}	2.42×10^{-7}	-
	B[b]F	3	3.40×10^{-7}	2.99×10^{-7}	3.79×10^{-7}	4.00×10^{-8}
	B[k]F	1	4.20×10^{-7}	4.20×10^{-7}	4.20×10^{-7}	-
	Total PAHs	3	8.39×10^{-7}	2.99×10^{-7}	1.46×10^{-6}	5.82×10^{-7}
Wisma	Flr	2	6.17×10^{-8}	5.31×10^{-8}	7.03×10^{-8}	1.22×10^{-8}
	Ant	4	9.31×10^{-8}	7.10×10^{-8}	1.54×10^{-7}	4.06×10^{-8}
	Flt	4	7.16×10^{-8}	4.80×10^{-8}	1.30×10^{-7}	3.88×10^{-8}
	Pyr	3	5.98×10^{-8}	4.18×10^{-8}	9.14×10^{-8}	2.74×10^{-8}
	B[a]A	1	2.62×10^{-7}	2.62×10^{-7}	2.62×10^{-7}	-
	Chr	1	2.19×10^{-7}	2.19×10^{-7}	2.19×10^{-7}	-
	B[b]F	3	3.44×10^{-7}	3.17×10^{-7}	3.66×10^{-7}	2.50×10^{-8}
	B[k]F	1	4.00×10^{-7}	4.00×10^{-7}	4.00×10^{-7}	-
	B[a]P	1	4.03×10^{-7}	4.03×10^{-7}	4.03×10^{-7}	-
	Total PAHs	4	8.20×10^{-7}	1.77×10^{-7}	1.37×10^{-6}	5.06×10^{-7}
KKKL	Ace	3	3.27×10^{-7}	4.67×10^{-8}	6.41×10^{-7}	2.99×10^{-7}
	Flr	5	2.95×10^{-7}	3.63×10^{-8}	8.91×10^{-7}	3.70×10^{-7}
	Ant	4	4.31×10^{-7}	6.82×10^{-8}	1.06×10^{-6}	4.62×10^{-7}
	Flt	4	2.86×10^{-7}	4.71×10^{-8}	9.70×10^{-7}	4.56×10^{-7}
	Pyr	4	3.53×10^{-7}	4.05×10^{-8}	9.08×10^{-7}	4.03×10^{-7}
	B[a]A	3	4.90×10^{-7}	1.37×10^{-7}	9.57×10^{-7}	4.22×10^{-7}
	Chr	5	1.98×10^{-7}	1.18×10^{-7}	2.89×10^{-7}	6.54×10^{-8}
	B[b]F	6	2.64×10^{-7}	1.48×10^{-7}	3.33×10^{-7}	7.47×10^{-8}

Preprints (www.preprints.org) | NOT PEER-REVIEWED | Posted: 18 January 2021 doi:10.20944/preprints202101.0362.v1

B[k]F	3	3.51×10^{-7}	2.85×10^{-7}	3.86×10^{-7}	5.71×10^{-8}
B[a]P	3	4.06×10^{-7}	2.13×10^{-7}	5.82×10^{-7}	1.85×10^{-7}
I[c]P	2	9.46×10^{-7}	8.10×10^{-7}	1.08×10^{-6}	1.93×10^{-7}
B[h]A	1	1.20×10^{-6}	1.20×10^{-6}	1.20×10^{-6}	-
B[g]P	1	7.15×10^{-7}	7.15×10^{-7}	7.15×10^{-7}	-
Total PAHs	6	2.81×10^{-6}	1.48×10^{-7}	9.94×10^{-6}	3.79×10^{-6}

Table 3: The factor loadings after PCA varimax-rotation at the study areas.

Variables	Factor 1	Factor 2	Factor 3	Factor 4
Fluorene	**0.955**	0.049	0.058	0.271
Anthracene	**0.970**	0.043	0.010	0.202
Fluoranthene	**0.976**	0.052	0.081	-0.080
Pyrene	**0.977**	0.031	0.025	0.186
Benzo(a)anthracene	**0.957**	0.258	0.036	-0.013
Chrysene	0.196	0.271	0.314	**0.884**
Benzo(b)fluoranthene	0.049	0.173	**0.954**	0.239
Benzo(k)fluoranthene	0.037	**0.952**	0.179	0.213
Benzo(a)pyrene	**0.757**	**0.629**	0.066	0.093
Eigen values	5.787	1.824	0.803	0.462
Variance (%)	64.301	20.267	8.926	5.133
Cumulative (%)	64.301	84.568	93.494	98.627
Sources of the pollutants	Natural gas and biomass burning	Urban traffic combustion	Combustion of heavy oil	Coal combustion

Average concentration of total PAHs was 1.74 ± 2.68 (range of 0.15 to 9.94) ng/m^3. This value is lower compared to other literatures. Liu, Man, Ma, Li, Wu and Peng [9] stated that the mean concentration of total PAHs in Guangzhou China from June 2012 until May 2013 was 33.89 (6.99-105.76) ng/m^3. Zhang, Cao, Li, Ho, Wang, Zhu and Wang [7] reported that average concentration of total quantified PAHs during whole sampling period at Huli in Xiamen was 10.10 ± 7.07 ng/m^3. Concentration of PAHs for background and peatland fire in Riau, Sumatra, Indonesia were 23.9 ± 2.53 ng/m^3 and (71.2 ± 0.36)×10^3 ng/m^3 as reported by Fujii, Iriana, Oda, Puriwigati, Tohno, Lestari, Mizohata and Huboyo [40]. The peatland fire PAHs concentration are much higher compared to our value due to the sampling area just 1.5 m away from the fire and the peatland fire emitted abundant of $PM_{2.5}$ aerosol. Khan, Latif, Lim, Amil, Jaafar, Dominick, Nadzir, Sahani and Tahir [4] reported that the average of total PAHs at UKM Bangi was 2.79 (0.21-12.08). Sulong, Latif, Sahani, Khan, Fadzil, Tahir, Mohamad, Sakai, Fujii and Othman [35] described the concentration of total PAHs in $PM_{2.5}$ during southwest monsoon (Jun-Sep), inter-monsoon I (Oct-Nov), northeast monsoon

(Dec-Mar), inter-monsoon II (Apr-May) and during haze episode in Kuala Lumpur were 2.51 ± 0.93 ng/m^3, 2.87 ± 0.14 ng/m^3, 1.37 ± 0.09 ng/m^3, 2.20 ± 0.71 ng/m^3 and 3.40 ± 0.68 ng/m^3 respectively. Jamhari, Sahani, Latif, Chan, Tan, Khan and Tahir [37] recorded that the total PAHs concentration in Kuala Lumpur and Petaling Jaya were 2.03 ± 0.69 ng/m^3 and 3.56 ± 1.07 ng/m^3 respectively. All these three values are not so different with our value, may due to the locations are from/nearby Kuala Lumpur.

Among of these three sampling sites, KKKL has the highest average concentration of total PAHs which is 2.18 ± 3.79 ng/m^3, followed by DBKL and Wisma with mean concentration of 0.84 ± 0.59 ng/m^3 and 0.82 ± 0.51 ng/m^3 respectively as shown in **Table 2**. Generally, the common PAHs that are found in all sampling sites are B[k]F, B[b]F, B[a]A, Chr, Pyr, Flr, Ant and Flt. B[a]P are found in Wisma and KKKL. At KKKL sampling site, there are 13 PAHs detected. The three highest concentration is B[h]A (1.20 ng/m^3), I[c]P (0.95 ± 0.19 ng/m^3) and followed by B[g]P (0.72 ng/m^3). The trend for mean concentration of PAHs in KKKL is B[h]A > I[c]P > B[g]P > B[a]A > Ant > B[a]P > Pyr > B[k]F > Ace > Flr > Flt > B[b]F > Chr. For DBKL, eight PAHs were detected with B[k]F (0.42 ng/m^3) as the highest mean concentration, followed by B[b]F 0.34 ± 0.04 ng/m^3 and Chr 0.24 ng/m^3. The trend for the mean concentration of PAHs in DBKL is B[k]F > B[b]F > Chr > B[a]A > Ant > Flt > Flr > Pyr. As for Wisma, the highest mean concentration is B[a]P and B[k]F (4.03×10^{-1} ng/m^3 and 0.40 ng/m^3 respectively), followed by and B[b]F with mean concentration of 0.34 ± 0.25×10^{-2} ng/m^3. There are nine PAHs detected in Wisma. The trend for the mean concentration of PAHs in Wisma was B[a]P > B[k]F > B[b]F > B[a]A > Chr > Ant > Flt > Flr > Pyr.

Preprints (www.preprints.org) | NOT PEER-REVIEWED | Posted: 18 January 2021 doi:10.20944/preprints202101.0362.v1

3.4 Identification of possible sources

3.4.1 Diagnostic Ratio (DR)

Application of Ant / (Ant + Phe) was not possible because no phenanthrene was detected in the samples. From **Table S2**, mean ratio of Flt to (Flt + Pyr) is 0.5459. This ratio value suggests that the PAHs has been released from coal, grass and wood burning as reported by Yunker, Macdonald, Vingarzan, Mitchell, Goyette and Sylvestre [49] and De La Torre-Roche, Lee and Campos-Díaz [39],Yunker, Macdonald, Vingarzan, Mitchell, Goyette and Sylvestre [49]. Similarly, ratio of B[a]A to (B[a]A + Chr) is 0.58 which implies that the PAHs emitted from wood burning activities as reported by Akyüz and Çabuk [57], Manoli, Kouras and Samara [48] and Yunker, Macdonald, Vingarzan, Mitchell, Goyette and Sylvestre [49]. Ratio of I[c]P to (I[c]P + B[g]P) obtained was 0.60. Brändli, Bucheli, Ammann, Desaules, Keller, Blum and Stahel [47] and Yunker, Macdonald, Vingarzan, Mitchell, Goyette and Sylvestre [49] suggested that this PAHs come from emission of coal, wood and grass burning, also from diesel. From ratio of B[a]P/B[g]P, the value of 0.82 emitted from traffic as proposed by Brändli, Bucheli, Ammann, Desaules, Keller, Blum and Stahel [47] and Yunker, Macdonald, Vingarzan, Mitchell, Goyette and Sylvestre [49]. The PAHs are estimated to come mainly from coal, grass and wood burning activities also from traffic emission. The high density of traffic in the sampling site is a potential cause in this regard and due to the wind speed and flow that brought the PAHs from coal and open burning near the sampling site.

3.4.2 PCA-MLR

PCA factor loadings obtained via the varimax rotation are shown in **Table 2**. The PCA analysis arranged the dataset of PAHs into four principal components (PCs) that control 98.63% of the data variance at Kuala Lumpur. Factor 1 (64.3% of the total variance) was highly loaded on Flu, Ant, Flt, Pyr, B[a]A and B[a]P, suggesting that the emissions are from natural gas and coal burning sources [21,58,59]. Ant, Pyr, B[a]A are typical indicator of wood combustion while B[a]P are come from emission of coal combustion [22]. Flt,

Preprints (www.preprints.org) | NOT PEER-REVIEWED | Posted: 18 January 2021 doi:10.20944/preprints202101.0362.v1

Pyr, B[a]A are tracers for the emission of natural gas [20,37]. Sulong, Latif, Sahani, Khan, Fadzil, Tahir, Mohamad, Sakai, Fujii and Othman [35] reported that Flu, Ant, Flt, Pyr are emission from natural gas and biomass burning. B[a]P is specific marker for vehicle and gasoline emission [21,22,35,37]. However, Factor 1 shows more tracer for emission from natural gas, coal and biomass burning. Factor 2 (20.27% of the total variance) was loaded with B[k]F and B[a]P, indicating that the emission come from vehicle and gasoline combustion. Higher level of B[k]F is suggested to indicate diesel vehicles [28] and B[a]P is specific marker for vehicle and gasoline emissions [21,22,35,37]. These emissions can be classified as urban traffic combustion. Factor 3 (8.93% of the total variance) was dominated by B[b]F (HMW PAH) are expelled from the combustion of heavy oil [21,35]. Factor 4 (5.13% of total variance) was dominated by Chr. Chr is a marker of coal combustion [22,28].

We also believed that these pollutants may be influent from neighboring country that has been emitted and carried by the wind to Malaysia. As reported, a major portion (about 70%) of the energy in China has been obtained from coal (https://www.worldatlas.com/articles/15-countries-most-dependent-on-coal-for-energy.html). Coal was also identified as the largest source of $PM_{2.5}$ bound -PAHs in Beijing [23]. Biomass burning also occurred potentially in the East Asian region e.g. Hong Kong and reported as a predominant source of PAHs in $PM_{2.5}$ [60]. From **Fig. S3**, the wind blew from the South China Sea and may carry all these pollutant from the mainland of China and other IndoChina countries. Back track trajectory of air mass was plotted to further observed the direction of wind-blown to the monitoring site. Back trajectory using HYSPLIT model as shown in **Fig. 2** depicts that the Northeast monsoon wind arrives in three months (**Fig. 2** (a) January, **Fig. 2** (b) February and **Fig. 2** (c) March) at the monitoring stations. **Figure 2 (a)** January shows there are four main cluster of back trajectories which cluster 1 blown from mainland China about 14%, cluster show 8%

Preprints (www.preprints.org) | NOT PEER-REVIEWED | Posted: 18 January 2021 doi:10.20944/preprints202101.0362.v1

blown from Indochina regions, cluster 3 shows 52% both from Taiwan and South China Seas region and cluster 4 shows 26% from Philippines region. **Figure 2 (b)** February and **Fig. 2 (c)** March show similar pattern where there are two main clusters of back trajectories which both clusters were blown from South China Sea region. Therefore, source of transboundary pollutants may also contribute from South China Sea activity.

The quantitative source apportionment of PAHs was determined using APCS-MLR procedure. The regression plot between PAHs from GC-FID and PAHs predicted by APCS shows a Signiant correlation (R^2 = 0.98). From **Fig. 3**, the identified factors were emission from natural gas and biomass burning (Factor 1), urban traffic combustion (Factor 2), combustion of heavy oil (Factor 3) and coal combustion (Factor 4). These four factors contributed 30% (Factor 1), 5% (Factor 2), 3% (Factor 3) and (Factor 4) 5% respectively and leaving 57% of the PAHs concentration as undefined. The percentage of undefined PAHs is higher because some of the variables were excluded, because the data is ≤ 30% from overall variables.

Preprints (www.preprints.org) | NOT PEER-REVIEWED | Posted: 18 January 2021 doi:10.20944/preprints202101.0362.v1

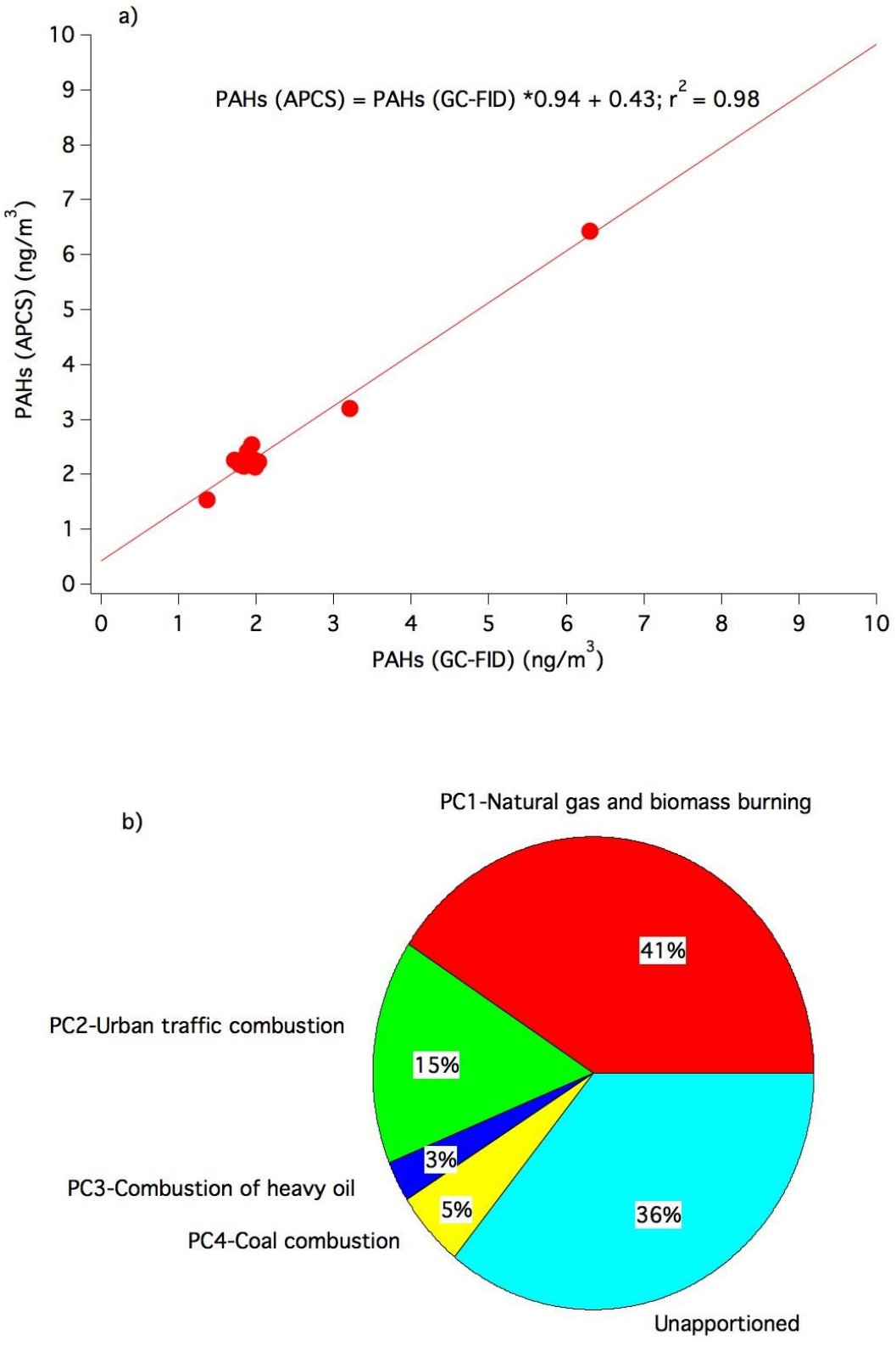

Figure 3: The percentage of predicted PAHs sources with the application of PCA-APCS in Kuala Lumpur.

Preprints (www.preprints.org) | NOT PEER-REVIEWED | Posted: 18 January 2021 doi:10.20944/preprints202101.0362.v1

3.5 Human exposure of PAH

3.5.1 Toxicity risk

BaP_{eq} was estimated via the multiplying the PAH concentration with the respective TEF value to estimate the toxicity of the compound by comparing them with the concentration of benzo(a)anthracene, B[a]P. **Table S8** shows that there is no BaPeq concentration that higher than B[a]P compound (1.63 ng/m^3). B[h]A also gives relatively high concentration of BaPeq, which is 1.20 ng/m^3. The total concentration of BaP_{eq} is 3.82 ng/m^3, with the average of 0.29 (range of 0.001-1.62) ng/m^3. This value is almost same with Sulong, Latif, Sahani, Khan, Fadzil, Tahir, Mohamad, Sakai, Fujii and Othman [35] study, whose reported that the total BaP_{eq} concentration in Kuala Lumpur during different monsoon seasons and haze episode was 0.266 ng/m^3. Liu, Man, Ma, Li, Wu and Peng [9] reported that mean concentration of total BaPeq in Guangzhou China was 6.69 (range of 0.96-22.46 ng/m^3), which is much higher compared to this study. This is due to the rapid industrialization and insufficient emission control in the sampling area, Guangzhou China. BaPeq (ng/m^3) was observed in China, Japan, South Korea, Vietnam and India with the value of 7.79 (range of 0.49-34.8), 0.288 (0.09-0.71), 1.21 (0.61-2.66), 4.44 (1.26-10.6) and 5.79 (0.95-19.0) ng/m^3 respectively [33]. From the total BaPeq, the lifetime lung cancer risk (LLCR) can be estimated. Zhang, *et al.* [61] stated that LLCR < 1.0×10^{-6}, 1.0×10^{-6} < LLCR < 1.0×10^{-4}, 1.0×10^{-4} < LLCR < 1.0×10^{-3}, 1.0×10^{-3} < LLCR < 1.0×10^{-1} and LLCR > 1.0×10^{-1} as very low cancer risk, low risk, moderate risk, high risk and very high risk, respectively. In this study, the calculated value is 3.32×10^{-4}, and is classified as moderate risk.

Preprints (www.preprints.org) | NOT PEER-REVIEWED | Posted: 18 January 2021 doi:10.20944/preprints202101.0362.v1

3.5.2 Carcinogenic exposure

3.5.2.1 Lifetime average daily dose

Carcinogenic lifetime average daily dose (LADD) concentrations for infant, toddler, children, adolescent and adult were shown in **Table S9.** The concentrations were followed the order of adult > toddler > adolescent > children > infant. Adult has the highest concentration which is 1.29×10^{-7} (range of 1.09×10^{-8} to 7.33×10^{-7}) mg/kg day followed by toddler, adolescent, children and infant with values of 7.17×10^{-8} (range of 6.08×10^{-9} to 4.08×10^{-7}), 5.92×10^{-8} (range of 5.02×10^{-9} to 3.37×10^{-7}), 5.51×10^{-8} (range of 4.67×10^{-9} to 3.14×10^{-7}) and 1.84×10^{-8} (range of 1.56×10^{-9} to 1.05×10^{-7}) mg/kg day respectively. From the **Table S9**, B[h]A has the highest concentration compared to other compounds in all age groups.

3.5.2.2 Excess lifetime cancer risk (ELCR)

From **Table S11 a)**, B[h]A in all age group has the highest ELCR value compared to other compounds, followed by B[a]P and I[c]P. These compounds have high molecular weight that has high stability and classified as carcinogenic. Mean concentration of the PAHs for all age groups followed the order of B[h]A > B[a]P > I[c]P > B[a]A > B[k]F > B[b]F > B[g]P > Ant > Chr > Ace > Flr > Pyr > Flt. Table ELCR shows that the pattern of the PAHs inhalation exposure is adult > children > adolescent > toddler > infant. Sulong, Latif, Sahani, Khan, Fadzil, Tahir, Mohamad, Sakai, Fujii and Othman [35] described that the cancer risk in their study followed the order of adult > toddler > adolescent > children > infant. The result for adults and children are similar compared to the current study in which adult has the highest value and infant has the lowest value of ILCR. Jamhari, Sahani, Latif, Chan, Tan, Khan and Tahir [37] also reported that adult has the highest ILCR value and infant has the lowest value of ILCR among the age groups. Adult has highest health risk compared

to others because adult is exposed to the carcinogen for long period of time compared to other age groups. It is possibly due to the longer of the exposure time as the concentration of carcinogenic element can accumulate in the body during such extended lifetime. However,the estimated cancer risk that have been calculated were considered insignificant and safe since the values in less than 1×10^{-6}.

From **Table S11 b)** shows that adult has the highest values of ELCR whereas infant has the lowest values of ELCR for each sampling sites. For DBKL, B[k]F has the highest ELCR values followed by B[b]F, B[a]A and Chr for each age groups. As for Wisma, for all age groups, B[a]P has the highest ELCR values followed by B[k]F, B[b]F and B[a]A. While for KKKL, B[h]A has the highest ELCR value followed by B[a]P, B[a]A and I[c]P for each age groups.

3.5.3 Non-carcinogenic exposure

3.6.3.1 Average daily dose (ADD) for non-carcinogenic exposure

Table S10 shows the ADD for non-cancer risk for infant, toddler, children, adolescent and adult. The ADD for average total PAHs followed order infant > toddler > adolescent > children > adult. Infant has the highest average of total PAHs while adult has the lowest ADD with value of 1.34×10^{-6} (range of 1.14×10^{-7} to 7.67×10^{-6}) and 3.91×10^{-7} (range of 3.32×10^{-8} to $2.23\times10^{-6)}$ mg/ kg day, respectively.

3.6.3.2 Hazard Quotient (HQ) and Hazard Index (HI)

For non-carcinogenic risk detection, Health Quotient (HQ) and Hazard Index (HI) are used. HQ are obtained by dividing ADD with R_fD values, while HI are estimated by summation of the HQ values for every group of age. As shown in **Table S12 a)**, the trend for average total PAHs HQ is infant > toddler > adolescent > children > adult. Infant has highest HQ value which is 3.92×10^{-4}, followed by toddler, adolescent, children and adult which has HQ value of 3.05×10^{-4}, 2.10×10^{-4}, 1.96×10^{-4} and 1.14×10^{-4}, respectively.

Preprints (www.preprints.org) | NOT PEER-REVIEWED | Posted: 18 January 2021 doi:10.20944/preprints202101.0362.v1

Comparing to other compound, HQ for B[a]P for all age groups is the highest, with value of $\times 10^{-3}$ to $\times 10^{-4}$. Khpalwak, Jadoon, Abdel-dayem and Sakugawa [22] observed HQ via inhalation route for the road and aerial dusts from Kabul and Jalalabad cities, Afghanistan. HQ estimated from three types of air particles such as road-dust Kabul, road-dust Jalalabad and aerial-dust Jalalabad were 2.99×10^{-9} (children) and 5.12×10^{-9} (adult), 1.42×10^{-9} (children) and 2.44×10^{-9} (adult), and 2.36×10^{-9} (children) and 1.38×10^{-9} (children) respectively. From **Table S12 b)**, the trends of HQ for all sampling sites are the same, which is infant > toddler > adolescent > children > adult. KKKL has the highest HQ of mean total PAHs in KKKL followed by Wisma and DBKL. For all age groups, HQ for B[a]P is the highest compared to other compounds in both KKKL and Wisma, while for DBKL, the highest HQ is Flt.

From the current study, HI for infant is the highest with value of 0.0043, followed with toddler, adolescent, children and adult with values of 0.0034, 0.0023, 0.0022 and 0.0013 respectively. The trend is also similar with the trend of HQ for each age group. Our results showed that none of the age group category were the risk of HI>1. All age groups showed HI values of 10^{-3}, which is lower than one (1). In addition, for every age groups, DBKL has the lowest HI values which is $\times 10^{-6}$ compared to Wisma and KKKL. Thus, non-carcinogenic health effect was less prominent at the studies areas.

4. Conclusion

In this study, concentration of OC_1, OC_2, OC_3, OC_4, OP, EC_1, EC_2 and EC_3 were determined by using IMPROVE_A protocol and then concentration of SOC was estimated. The average concentrations of OC, EC and SOC were 6.88 ± 4.94 μg/m^3, 3.68 ± 1.58 μg/m^3 and 2.33 μg/m^3, respectively. Average concentration of WSOC was 2.73 ± 2.17 (range of 0.63-9.12) μg/m^3. This study also reports that the average concentration of total PAHs in Kuala Lumpur City was 1.77 ± 2.74 ng/m^3. The PAHs particles were

 doi:10.20944/preprints202101.0362.v1

estimated mainly come from natural gas and biomass burning (coal, grass and wood burning), and from fuel combustion. From the concentrations of PAHs obtained, health risk assessment for age groups of infants, toddler, children, adolescent and adult were conducted. For the toxicity risk, the total concentration of BaP_{eq} is 3.82 ng/m^3, with the average of 0.29 (range of 0.001-1.62) ng/m^3. Adult has the highest ELCR whereas infant has the lowest ELCR. However, carcinogenic risks were insignificant because the values were not in the range of 1.00×10^{-6} to 1.00×10^{-4}. For non-carcinogenic risk, infant has highest HQ value which is 3.92×10^{-4}, followed by toddler, adolescent, children and adult which has HQ value of 3.05×10^{-4}, 2.10×10^{-4}, 1.96×10^{-4} and 1.14×10^{-4} respectively. Hazard Index (HI) for all age groups were less than one (<1), means that no substantial non-cancerous risk is present. Although the health risk assessment that have been done shows no significant health risk for both carcinogenic and non- carcinogenic risk, precautionary measures must be taken to reduce the PAHs exposure. To better elucidate potential PAH emission sources, the use of multivariate source apportionment modeling e.g. PMF with long-term monitoring data would be needed. In future study, we will consider a long term of the sampling and also the breathing zone or level for the $PM_{2.5}$ sampling to avoid the bias in risk analysis. To reduce emission from biomass burning and vehicles combustion, the government should take actions against those who doing open burning or uncontrolled biomass burning and encourage public to use public transport rather than drive their own vehicle.

Acknowledgement

This research is supported by Fundamental Research Grant Scheme (FRGS) FP099-2019A. We also sincerely acknowledge the Department of Environment (DOE) and Pakar Scieno TransWater for providing us the filter samples. The authors are thankful to Dr. Tay Kheng Soo for his guidance to synthesize the magnetic nanoparticles. The authors

would also like to acknowledge Mrs. Ruhaida Bahru and Mrs Nor Lela Md Ali for their assistance on instrumentation and laboratory facilities, as well as Mr. Mohd Hazni Abdul Taib and the other laboratory staff. The data of the Hysplit model were available at ftp://arlftp.arlhq. noaa.gov/pub/archives/reanalysis. The authors gratefully acknowledge the NOAA Air Resources Laboratory (ARL) for the provision of the Hysplit transport and dispersion model and/or READY website (http://www.ready.noaa.gov) used in this publication.

References

1. Brauer, M.; Freedman, G.; Frostad, J.; van Donkelaar, A.; Martin, R.V.; Dentener, F.; Dingenen, R.v.; Estep, K.; Amini, H.; Apte, J.S., et al. Ambient Air Pollution Exposure Estimation for the Global Burden of Disease 2013. *Environ. Sci. Technol.* **2016**, *50*, 79-88, doi:10.1021/acs.est.5b03709.
2. Cohen, A.J.; Brauer, M.; Burnett, R.; Anderson, H.R.; Frostad, J.; Estep, K.; Balakrishnan, K.; Brunekreef, B.; Dandona, L.; Dandona, R., et al. Estimates and 25-year trends of the global burden of disease attributable to ambient air pollution: an analysis of data from the Global Burden of Diseases Study 2015. *The Lancet* **2017**, *389*, 1907-1918, doi:10.1016/S0140-6736(17)30505-6.
3. WHO. *World Health Organization. Global urban ambient air pollution database (update 2016).* World Health Organization, 2016.
4. Khan, M.F.; Latif, M.T.; Lim, C.H.; Amil, N.; Jaafar, S.A.; Dominick, D.; Nadzir, M.S.M.; Sahani, M.; Tahir, N.M. Seasonal effect and source apportionment of polycyclic aromatic hydrocarbons in PM2.5. *Atmos. Environ.* **2015**, *106*, 178-190, doi:10.1016/j.atmosenv.2015.01.077.
5. Liu, X.; Schnelle-Kreis, J.; Schloter-Hai, B.; Ma, L.; Tai, P.; Cao, X.; Yu, C.; Adam, T.; Zimmermann, R. Analysis of PAHs Associated with PM10 and PM2.5 from Different Districts in Nanjing. *Aerosol Air Qual. Res.* **2019**, *19*, 2294-2307, doi:10.4209/aaqr.2019.06.0301.
6. Omar, N.Y.M.; Mon, T.C.; Rahman, N.A.; Abas, M.R.B. Distributions and health risks of polycyclic aromatic hydrocarbons (PAHs) in atmospheric aerosols of Kuala Lumpur, Malaysia. *Sci. Total Environ.* **2006**, *369*, 76-81, doi:10.1016/j.scitotenv.2006.04.032.
7. Zhang, N.; Cao, J.; Li, L.; Ho, S.S.H.; Wang, Q.; Zhu, C.; Wang, L. Characteristics and source identification of polycyclic aromatic hydrocarbons and n-alkanes in PM2.5 in Xiamen. *Aerosol Air Qual. Res.* **2018**, *18*, 1673-1683, doi:10.4209/aaqr.2017.11.0493.
8. WHO. World Health Organization. Particulate Matter, Chapter 7.3. WHO Regional Publications. Copenhagen, Denmark. In 2000.
9. Liu, J.; Man, R.; Ma, S.; Li, J.; Wu, Q.; Peng, J. Atmospheric levels and health risk of polycyclic aromatic hydrocarbons (PAHs) bound to PM2.5 in Guangzhou, China. *Mar. Pollut. Bull.* **2015**, *100*, 134-143, doi:10.1016/j.marpolbul.2015.09.014.
10. Seinfield, J.H.; Pandis, S.N. *Atmospheric chemistry and physics: From air pollution to climate change.*; 2016.
11. Wang, J.; Ogawa, S. Effects of meteorological conditions on PM2.5 concentrations in Nagasaki, Japan. *Int. J. Environ. Res. Public Health* **2015**, *12*, 9089-9101, doi:10.3390/ijerph120809089.

12. Dominick, D.; Latif, M.T.; Juneng, L.; Khan, M.F.; Amil, N.; Mead, M.I.; Nadzir, M.S.M.; Moi, P.S.; Samah, A.A.; Ashfold, M.J. Characterisation of particle mass and number concentration on the east coast of the Malaysian Peninsula during the northeast monsoon. *Atmos. Environ.* **2015**, *117*, 187-199, doi:10.1016/j.atmosenv.2015.07.018.
13. Farren, N.J.; Dunmore, R.E.; Mead, M.I.; Mohd Nadzir, M.S.; Samah, A.A.; Phang, S.M.; Bandy, B.J.; Sturges, W.T.; Hamilton, J.F. Chemical characterisation of water-soluble ions in atmospheric particulate matter on the east coast of Peninsular Malaysia. *Atmos. Chem. Phys.* **2019**, *19*, 1537-1553, doi:10.5194/acp-19-1537-2019.
14. Khan, M.F.; Latif, M.T.; Amil, N.; Juneng, L.; Mohamad, N.; Nadzir, M.S.M.; Hoque, H.M.S. Characterization and source apportionment of particle number concentration at a semi-urban tropical environment. *Environ. Sci. Pollut. Res.* **2015**, *22*, 13111-13126, doi:10.1007/s11356-015-4541-4.
15. Nadzir, M.S.M.; Lin, C.Y.; Khan, M.F.; Latif, M.T.; Dominick, D.; Hamid, H.H.A.; Mohamad, N.; Maulud, K.N.A.; Wahab, M.I.A.; Kamaludin, N.F., et al. Characterization of rainwater chemical composition after a Southeast Asia haze event: insight of transboundary pollutant transport during the northeast monsoon. *Environ. Sci. Pollut. Res.* **2017**, *24*, 15278-15290, doi:10.1007/s11356-017-9131-1.
16. Wu, C.; Yu, J.Z. Determination of primary combustion source organic carbon-to-elemental carbon (OC/EC) ratio using ambient OC and EC measurements: secondary OC-EC correlation minimization method. *Atmos. Chem. Phys.* **2016**, *16*, 5453-5465, doi:10.5194/acp-16-5453-2016.
17. Rajput, P.; Sarin, M.; Kundu, S.S. Atmospheric particulate matter (PM2.5), EC, OC, WSOC and PAHs from NE–Himalaya: abundances and chemical characteristics. *Atmos. Pollut. Res.* **2013**, *4*, 214-221, doi:10.5094/APR.2013.022.
18. Zhang, H.; Ying, Q. Secondary organic aerosol from polycyclic aromatic hydrocarbons in Southeast Texas. *Atmos. Environ.* **2012**, *55*, 279-287, doi:10.1016/j.atmosenv.2012.03.043.
19. Ding, X.; Wang, X.-M.; Gao, B.; Fu, X.-X.; He, Q.-F.; Zhao, X.-Y.; Yu, J.-Z.; Zheng, M. Tracer-based estimation of secondary organic carbon in the Pearl River Delta, south China. *J. Geophys. Res.* **2012**, *117*, doi:10.1029/2011jd016596.
20. Chiu, T.R.; Khan, M.F.; Latif, M.T.; Mohd Nadzir, M.S.; Abdul Hamid, H.H.; Yusoff, H.; Mohd Ali, M. Distribution of Polycyclic Aromatic Hydrocarbons (PAHs) in Surface Sediments of Langkawi Island, Malaysia. *Sains Malays.* **2018**, *47(5)*, 871-882., doi:10.17576/jsm-2018-4705-02.
21. Harrison, R.M.; Smith, D.J.T.; Luhana, L. Source Apportionment of Atmospheric Polycyclic Aromatic Hydrocarbons Collected from an Urban Location in Birmingham, U.K. *Environmental Science and Technology* **1996**, *30*, 825-832, doi:10.1021/es950252d.
22. Khpalwak, W.; Jadoon, W.A.; Abdel-dayem, S.M.; Sakugawa, H. Polycyclic aromatic hydrocarbons in urban road dust, Afghanistan: Implications for human health. *Chemosphere* **2019**, *218*, 517-526, doi:10.1016/j.chemosphere.2018.11.087.
23. Yu, Q.; Yang, W.; Zhu, M.; Gao, B.; Li, S.; Li, G.; Fang, H.; Zhou, H.; Zhang, H.; Wu, Z., et al. Ambient PM2.5-bound polycyclic aromatic hydrocarbons (PAHs) in rural Beijing: Unabated with enhanced temporary emission control during the 2014 APEC summit and largely aggravated after the start of wintertime heating. *Environmental Pollution* **2018**, *238*, 532-542, doi:10.1016/j.envpol.2018.03.079.
24. Peltonen, K.; Kuljukka, T. Air sampling and analysis of polycyclic aromatic hydrocarbons. *J. Chromatogr. A* **1995**, *710*, 93-108, doi:10.1016/0021-9673(95)00207-4.
25. Gao, B.; Yu, J.-Z.; Li, S.-X.; Ding, X.; He, Q.-F.; Wang, X.-M. Roadside and rooftop measurements of polycyclic aromatic hydrocarbons in PM2.5 in urban Guangzhou: Evaluation of vehicular and regional combustion source contributions. *Atmos. Environ.* **2011**, *45*, 7184-7191, doi:10.1016/j.atmosenv.2011.09.005.
26. Pongpiachan, S.; Tipmanee, D.; Khumsup, C.; Kittikoon, I.; Hirunyatrakul, P. Assessing risks to adults and preschool children posed by PM2.5-bound polycyclic aromatic

hydrocarbons (PAHs) during a biomass burning episode in Northern Thailand. *Sci. Total Environ.* **2015**, *508*, 435-444, doi:10.1016/j.scitotenv.2014.12.019.

27. Wang, J.; Geng, N.B.; Xu, Y.F.; Zhang, W.D.; Tang, X.Y.; Zhang, R.Q. PAHs in PM2.5 in Zhengzhou: concentration, carcinogenic risk analysis, and source apportionment. *Environ. Monit. Assess.* **2014**, *186*, 7461-7473, doi:10.1007/s10661-014-3940-1.
28. Liu, Y.; Chen, L.; Huang, Q.-h.; Li, W.-y.; Tang, Y.-j.; Zhao, J.-f. Source apportionment of polycyclic aromatic hydrocarbons (PAHs) in surface sediments of the Huangpu River, Shanghai, China. *Sci. Total Environ.* **2009**, *407(8)*, 2931-2938, doi:10.1016/j.scitotenv.2008.12.046.
29. Goel, A.; Ola, D.; Veetil, A.V. Burden of disease for workers attributable to exposure through inhalation of PPAHs in RSPM from cooking fumes. *Environ. Sci. Pollut. Res.* **2019**, *26*, 8885-8894, doi:10.1007/s11356-019-04242-x.
30. Li, H.; Li, H.; Zhang, L.; Cheng, M.; Guo, L.; He, Q.; Wang, X.; Wang, Y. High cancer risk from inhalation exposure to PAHs in Fenhe Plain in winter: A particulate size distribution-based study. *Atmos. Environ.* **2019**, *216*, 116924, 116921-116911, doi:10.1016/j.atmosenv.2019.116924.
31. Zhang, Y.; Tao, S.; Shen, H.; Ma, J. Inhalation exposure to ambient polycyclic aromatic hydrocarbons and lung cancer risk of Chinese population. *Proc. Natl. Acad. Sci.* **2009**, *106*, 21063-21067, doi:10.1073/pnas.0905756106.
32. Sarkar, S.; Khillare, P. Profile of PAHs in the inhalable particulate fraction: source apportionment and associated health risks in a tropical megacity. *Environ. Monit. Assess.* **2013**, *185*, 1199-1213, doi:10.1007/s10661-012-2626-9.
33. Hong, W.-J.; Jia, H.; Ma, W.-L.; Sinha, R.K.; Moon, H.-B.; Nakata, H.; Minh, N.H.; Chi, K.H.; Li, W.-L.; Kannan, K. Distribution, fate, inhalation exposure and lung cancer risk of atmospheric polycyclic aromatic hydrocarbons in some Asian countries. *Environ. Sci. Technol.* **2016**, *50*, 7163-7174, doi:10.1021/acs.est.6b01090.
34. Khan, M.F.; Latif, M.T.; Saw, W.H.; Amil, N.; Nadzir, M.S.M.; Sahani, M.; Tahir, N.M.; Chung, J.X. Fine particulate matter in the tropical environment: monsoonal effects, source apportionment, and health risk assessment. *Atmos. Chem. Phys.* **2016a**, *16*, 597-617, doi:10.5194/acp-16-597-2016.
35. Sulong, N.A.; Latif, M.T.; Sahani, M.; Khan, M.F.; Fadzil, M.F.; Tahir, N.M.; Mohamad, N.; Sakai, N.; Fujii, Y.; Othman, M. Distribution, sources and potential health risks of polycyclic aromatic hydrocarbons (PAHs) in PM2.5 collected during different monsoon seasons and haze episode in Kuala Lumpur. *Chemosphere* **2019**, *219*, 1-14, doi:10.1016/j.chemosphere.2018.11.195.
36. Hopke, P.K. Review of receptor modeling methods for source apportionment. *J. Air Waste Manag. Assoc.* **2016**, *66*, 237-259, doi:10.1080/10962247.2016.1140693.
37. Jamhari, A.A.; Sahani, M.; Latif, M.T.; Chan, K.M.; Tan, H.S.; Khan, M.F.; Tahir, N.M. Concentration and source identification of polycyclic aromatic hydrocarbons (PAHs) in PM10 of urban, industrial and semi-urban areas in Malaysia. *Atmos. Environ.* **2014**, *86*, 16-27, doi:10.1016/j.atmosenv.2013.12.019.
38. Worldometers. Malaysia Population (access date 31 December 2019). Availabe online: https://www.worldometers.info/world-population/malaysia-population/ (accessed on
39. De La Torre-Roche, R.J.; Lee, W.Y.; Campos-Díaz, S.I. Soil-borne polycyclic aromatic hydrocarbons in El Paso, Texas: analysis of a potential problem in the United States/Mexico border region. *J. Hazard. Mater.* **2009**, *163*, 946-958, doi:10.1016/j.jhazmat.2008.07.089.
40. Fujii, Y.; Iriana, W.; Oda, M.; Puriwigati, A.; Tohno, S.; Lestari, P.; Mizohata, A.; Huboyo, H.S. Characteristics of carbonaceous aerosols emitted from peatland fire in Riau, Sumatra, Indonesia. *Atmos. Environ.* **2014**, *87*, 164-169, doi:10.1016/j.atmosenv.2014.01.037.
41. Khan, M.F.; Sulong, N.A.; Latif, M.T.; Nadzir, M.S.M.; Amil, N.; Hussain, D.F.M.; Lee, V.; Hosaini, P.N.; Shaharom, S.; Yusoff, N.A.Y.M. Comprehensive assessment of PM2.5

physicochemical properties during the Southeast Asia dry season (southwest monsoon). *J. Geophys. Res. Atmos.* **2016b**, *121*, 14589-14611, doi:10.1002/2016JD025894.

42. Turpin, B.J.; Huntzicker, J.J. Secondary formation of organic aerosol in the Los Angeles basin: A descriptive analysis of organic and elemental carbon concentrations. *Atmos. Environ.* **1991**, *25*, 207-215, doi:https://doi.org/10.1016/0960-1686(91)90291-E.
43. Turpin, B.J.; Lim, H.-J. Species Contributions to PM2.5 Mass Concentrations: Revisiting Common Assumptions for Estimating Organic Mass. *Aerosol Sci. Technol.* **2001**, *35*, 602-610, doi:10.1080/02786820119445.
44. Khan, M.F.; Shirasuna, Y.; Hirano, K.; Masunaga, S. Characterization of PM2.5, PM2.5–10 and PM>10 in ambient air, Yokohama, Japan. *Atmos. Res.* **2010**, *96*, 159-172, doi:https://doi.org/10.1016/j.atmosres.2009.12.009.
45. Thuy, N.T.T.; Dung, N.T.; Sekiguchi, K.; Yamaguchi, R.; Thuy, L.B.; Hien, N.T.T. Levels and water soluble organic carbon of atmospheric nanoparticles in a location of Ha Noi, Vietnam. *Vietnam J. Sci. Technol.* **2017**, *55*, 745-755, doi:10.15625/2525-2518/55/6/9618.
46. Tay, K.S.; Rahman, N.A.; Abas, M.R.B. Magnetic nanoparticle assisted dispersive liquid–liquid microextraction for the determination of 4-n-nonylphenol in water. *Anal. Methods* **2013**, *5*, 2933-2938, doi:10.1039/C3AY00001J.
47. Brändli, R.C.; Bucheli, T.D.; Ammann, S.; Desaules, A.; Keller, A.; Blum, F.; Stahel, W.A. Critical evaluation of PAH source apportionment tools using data from the Swiss soil monitoring network. *J. Environ. Monit.* **2008**, *10*, 1278-1286, doi:10.1039/B807319H.
48. Manoli, E.; Kouras, A.; Samara, C. Profile analysis of ambient and source emitted particle-bound polycyclic aromatic hydrocarbons from three sites in northern Greece. *Chemosphere* **2004**, *56*, 867-878, doi:10.1016/j.chemosphere.2004.03.013.
49. Yunker, M.B.; Macdonald, R.W.; Vingarzan, R.; Mitchell, R.H.; Goyette, D.; Sylvestre, S. PAHs in the Fraser River basin: a critical appraisal of PAH ratios as indicators of PAH source and composition. *Org. Geochem.* **2002**, *33*, 489-515, doi:10.1016/S0146-6380(02)00002-5.
50. Mehmet, A.; Hasan, Ç. Gas-particle partitioning and seasonal variation of polycyclic aromatic hydrocarbons in the atmosphere of Zonguldak, Turkey. *Sci. Total Environ.* **2010**, *408*, 5550-5558, doi:10.1016/j.scitotenv.2010.07.063.
51. Thurston, G.D.; Spengler, J.D. A quantitative assessment of source contributions to inhalable particulate matter pollution in metropolitan Boston. *Atmos. Environ.* **1985**, *19*, 9-25, doi:10.1016/0004-6981(85)90132-5.
52. Alias, N.F.; Khan, M.F.; Sairi, N.A.; Zain, S.M.; Suradi, H.; Rahim, H.A.; Banerjee, T.; Bari, M.A.; Othman, M.; Latif, M.T. Characteristics, Emission Sources, and Risk Factors of Heavy Metals in PM2.5 from Southern Malaysia. *ACS Earth and Space Chemistry* **2020**, *4*, 1309-1323, doi:10.1021/acsearthspacechem.0c00103.
53. USEPA. United States Environmental Protection Agency. Risk Assessment Guidance for Superfund Volume 1, Human Health Evaluation Manual (Part A) Interim Final.Office of Emergency and Remedial Response U.S. Environmental Protection Agency Washington, D.C. 1989.
54. USEPA. United States Environmental Protection Agency. Risk Assessment Guidance for Superfund (RAGS), Volume 1, Human Health Evaluation Manual (Part F, Supplemental Guidance for Inhalation Risk Assessment). Office of Superfund Remediation and Technology Innovation Washington DC: 2009.
55. Gao, J.; Wang, K.; Wang, Y.; Liu, S.; Zhu, C.; Hao, J.; Liu, H.; Hua, S.; Tian, H. Temporal-spatial characteristics and source apportionment of PM2.5 as well as its associated chemical species in the Beijing-Tianjin-Hebei region of China. *Environmental Pollution* **2018**, *233*, 714-724, doi:10.1016/j.envpol.2017.10.123.
56. Arfaeina, H.; Hashemi, S.E.; Alamohoda, A.A.; Kermani, M. Evaluation of organic carbon, elemental carbon, and water soluble organic carbon concentration in PM2. 5 in the

ambient air of Sina Hospital district, Tehran, Iran. *J. adv. environ. health res.* **2016**, *4*, 95-101, doi:10.22102/jaehr.2016.40221.

57. Akyüz, M.; Çabuk, H. Gas–particle partitioning and seasonal variation of polycyclic aromatic hydrocarbons in the atmosphere of Zonguldak, Turkey. *Sci. Total Environ.* **2010**, *408*, 5550-5558, doi:https://doi.org/10.1016/j.scitotenv.2010.07.063.
58. Guo, X.; Li, C.; Gao, Y.; Tang, L.; Briki, M.; Ding, H.; Ji, H. Sources of organic matter (PAHs and n-alkanes) in PM2.5 of Beijing in haze weather analyzed by combining the C-N isotopic and PCA-MLR analyses. *Environmental Science: Processes and Impacts* **2016**, *18*, 314-322, doi:10.1039/c6em00037a.
59. Simcik, M.F.; Zhang, H.; Eisenreich, S.J.; Franz, T.P. Urban Contamination of the Chicago/Coastal Lake Michigan Atmosphere by PCBs and PAHs during AEOLOS. *Environ. Sci. Technol.* **1997**, *31*, 2141-2147, doi:10.1021/es9609765.
60. Ma, Y.; Cheng, Y.; Qiu, X.; Lin, Y.; Cao, J.; Hu, D. A quantitative assessment of source contributions to fine particulate matter (PM2.5)-bound polycyclic aromatic hydrocarbons (PAHs) and their nitrated and hydroxylated derivatives in Hong Kong. *Environmental Pollution* **2016**, *219*, 742-749, doi:10.1016/j.envpol.2016.07.034.
61. Zhang, Y.; Zheng, H.; Zhang, L.; Zhang, Z.; Xing, X.; Qi, S. Fine particle-bound polycyclic aromatic hydrocarbons (PAHs) at an urban site of Wuhan, central China: Characteristics, potential sources and cancer risks apportionment. *Environmental Pollution* **2019**, *246*, 319-327, doi:10.1016/j.envpol.2018.11.111.

CRediT author statement

Hamidah Suradi: Formal analysis, Visualization, Writing- Original draft preparation **Md Firoz Khan:** Conceptualization, Formal analysis, Visualization, Writing- review and editing **Nor Asrina Sairi:** Validation, Writing- review and editing **Haasyimah Ab Rahim:** Writing- review and editing **Yusuke Fujii:** Validation, Writing- review and editing **Kai Qin:** Writing- review and editing **Md. Aynul Bari:** Writing- review and editing **Murnira Othman:** Writing- review and editing **Mohd Talib Latif:** Validation, Writing- review and editing